First detection of cyanamide (NH2CN) towards solar-type protostars

A&A 612, A107 (2018)
https://doi.org/10.1051/0004-6361/201732346

Astronomy & Astrophysics

First detection of cyanamide (NH_2CN) towards solar-type protostars

A. Coutens[1], E. R. Willis[2], R. T. Garrod[2], H. S. P. Müller[3], T. L. Bourke[4], H. Calcutt[5], M. N. Drozdovskaya[6], J. K. Jørgensen[5], N. F. W. Ligterink[7], M. V. Persson[8], G. Stéphan[2], M. H. D. van der Wiel[9], E. F. van Dishoeck[7,10], and S. F. Wampfler[6]

[1] Laboratoire d'Astrophysique de Bordeaux, Univ. Bordeaux, CNRS, B18N, allée Geoffroy Saint-Hilaire, 33615 Pessac, France
e-mail: audrey.coutens@u-bordeaux.fr
[2] Departments of Chemistry and Astronomy, University of Virginia, Charlottesville, VA 22904, USA
[3] I. Physikalisches Institut, Universität zu Köln, Zülpicher Str. 77, 50937 Köln, Germany
[4] SKA Organization, Jodrell Bank Observatory, Lower Withington, Macclesfield, Cheshire SK11 9DL, UK
[5] Centre for Star and Planet Formation, Niels Bohr Institute and Natural History Museum of Denmark, University of Copenhagen, Øster Voldgade 5-7, 1350 Copenhagen K, Denmark
[6] Center for Space and Habitability, Universität Bern, Sidlerstr. 5, 3012 Bern, Switzerland
[7] Leiden Observatory, Leiden University, PO Box 9513, 2300 RA Leiden, The Netherlands
[8] Department of Space, Earth and Environment, Chalmers University of Technology, Onsala Space Observatory, 439 92 Onsala, Sweden
[9] ASTRON Netherlands Institute for Radio Astronomy, PO Box 2, 7990 AA Dwingeloo, The Netherlands
[10] Max-Planck Institut für Extraterrestrische Physik (MPE), Giessenbachstr. 1, 85748 Garching, Germany

Received 22 November 2017 / Accepted 26 December 2017

ABSTRACT

Searches for the prebiotically relevant cyanamide (NH_2CN) towards solar-type protostars have not been reported in the literature. We present here the first detection of this species in the warm gas surrounding two solar-type protostars, using data from the Atacama Large Millimeter/Submillimeter Array Protostellar Interferometric Line Survey (PILS) of IRAS 16293–2422 B and observations from the IRAM Plateau de Bure Interferometer of NGC 1333 IRAS2A. We also detected the deuterated and ^{13}C isotopologs of NH_2CN towards IRAS 16293–2422 B. This is the first detection of NHDCN in the interstellar medium. Based on a local thermodynamic equilibrium analysis, we find that the deuteration of cyanamide (~1.7%) is similar to that of formamide (NH_2CHO), which may suggest that these two molecules share NH_2 as a common precursor. The NH_2CN/NH_2CHO abundance ratio is about 0.2 for IRAS 16293–2422 B and 0.02 for IRAS2A, which is comparable to the range of values found for Sgr B2. We explored the possible formation of NH_2CN on grains through the NH_2 + CN reaction using the chemical model MAGICKAL. Grain-surface chemistry appears capable of reproducing the gas-phase abundance of NH_2CN with the correct choice of physical parameters.

Key words. astrochemistry – astrobiology – ISM: molecules – stars: protostars – ISM: individual objects: IRAS 16293-2422 – ISM: individual objects: NGC 1333 IRAS2A

1. Introduction

Cyanamide (NH_2CN) is one of the rare interstellar molecules that contain two atoms of nitrogen. This species is thought to be relevant for prebiotic chemistry: in liquid water it may convert into urea, an important molecule in biological processes (Kilpatrick 1947). Its isomer carbodiimide (HNCNH) can be formed from NH_2CN in photochemically and thermally induced reactions in interstellar ice analogs (Duvernay et al. 2005). Molecules with the carbodiimide moiety (–NCN–) find use in various biological processes, among which the assembly of amino acids into peptides (see Williams & Ibrahim 1981 for an overview). Although this molecule has been detected in other galaxies, such as NGC 253 and M82 (Martín et al. 2006; Aladro et al. 2011), only two detections are mentioned in our Galaxy, in the massive star-forming regions Sgr B2 (Turner et al. 1975) and Orion KL (White et al. 2003).

Molecules formed early during the star formation process may be incorporated into comets or asteroids and delivered to planets during heavy bombardment periods, similar to that experienced by the young Earth (Raymond et al. 2004). Here, we report the detection of cyanamide towards two solar-type protostars, IRAS 16293–2422 (hereafter IRAS 16293) and NGC 1333 IRAS2A (hereafter IRAS2A). These two low-mass protostars are known to harbor a very rich chemistry in their inner regions (e.g., Bottinelli et al. 2004; Jørgensen et al. 2005). This can be explained by the thermal desorption of the numerous and complex species formed in the icy mantles of the grains. The detection presented in this work complements the list of molecules of prebiotic interest such as glycolaldehyde, formamide, and methyl isocyanate discovered in low-mass protostars (Jørgensen et al. 2012; Kahane et al. 2013; Maury et al. 2014; Coutens et al. 2015; Ligterink et al. 2017; Martín-Doménech et al. 2017). We also detected the deuterated form of cyanamide, NHDCN, for the first time in the interstellar medium.

2. Observations

To search for cyanamide, we used data obtained with the Atacama Large Millimeter/Submillimeter Array (ALMA) for

IRAS 16293 and with the IRAM Plateau de Bure Interferometer (PdBI) for IRAS2A.

The ALMA data are part of the Protostellar Interferometric Line Survey (PILS) program[1], a large spectral survey of IRAS 16293 observed in Cycle 2 between 329.1 and 362.9 GHz at a spatial resolution of about 0.5″ and a spectral resolution of ∼0.2 km s^{-1}. The observations and their reduction are presented in Jørgensen et al. (2016). The data reach a sensitivity of about 4–5 mJy beam^{-1} km s^{-1}.

The PdBI data of the low-mass protostar IRAS2A were obtained with the WIDEX correlator in the framework of several programs (V010, V05B, W00A, and X060). The data reduction of each dataset is described in Coutens et al. (2014, 2015) and Persson et al. (2014). They cover the spectral ranges 223.5–227.1, 240.2–243.8, and 315.5–319.1 GHz with a spectral resolution of 1.95 MHz (∼1.8–2.6 km s^{-1}). The angular resolution is about 1.2″ × 1.0″ at 225 GHz, 1.4″ × 1.0″ at 242 GHz, and 0.9″ × 0.8″ at 317 GHz. The rms are ∼5–6 mJy beam^{-1} km s^{-1} or lower.

The spectroscopic data used here for cyanamide and its ^{13}C isotopolog come from the spectroscopic catalogs Jet Propulsion Laboratory (JPL, Pickett et al. 1998; Read et al. 1986) and Cologne Database for Molecular Spectroscopy (CDMS, Müller et al. 2001, 2005; Kraśnicki et al. 2011). The spectroscopy of NHDCN was studied by Kisiel et al. (2013). Carbodiimide spectroscopic information comes from the CDMS (Birk et al. 1989; Jabs et al. 1997).

3. Results

The CASSIS[2] software was used to search for and identify the lines of NH_2CN and its isotopologs towards IRAS 16293 and IRAS2A. Synthetic spectra were produced and compared with the observations to identify the lines. Potential blending with other species from the CDMS or JPL catalogs was checked. Column densities were determined assuming local thermodynamic equilibrium (LTE), which is reasonable for the inner regions of low-mass protostellar envelopes owing to their very high densities ($\gtrsim 10^{10}$ cm^{-3}, Jørgensen et al. 2016).

3.1. Analyses of cyanamide and carbodiimide

For the binary IRAS 16293, 11 unblended lines of the main cyanamide isotopolog are detected towards source B (see Fig. 2) at the full-beam offset position analyzed in previous studies (Coutens et al. 2016; Lykke et al. 2017; Ligterink et al. 2017). No clear detection could be obtained towards IRAS 16293 A, where the lines are broader (≥2 km s^{-1}). Maps indicate that the emission of this species arises from the warm inner regions around the B component (see Fig. 1), similarly to other complex organic molecules (Baryshev et al. 2015; Jørgensen et al. 2016). This species also appears to be strongly affected by absorption against the strong continuum similarly to formamide (Coutens et al. 2016, see their Fig. 1). The deep absorptions at the continuum peak and half-beam offset positions are clearly seen for all the lines (see Fig. B.1). Although a LTE model with a lower excitation temperature of 100 K is in relatively good agreement with the observations (see Fig. 2), a temperature of 300 K is a more appropriate fit. This is consistent with the temperature derived for other species with high binding energies such as glycolaldehyde, ethylene glycol, and formamide (see discussion in Jørgensen et al. 2018). At the full-beam offset position, a column density of ≥7 × 10^{13} cm^{-2} is derived for an excitation temperature of 300 K (≥5 × 10^{13} cm^{-2} for 100 K) and a source size of 0.5″. It should be noted that this column density can only be considered as a lower limit because of the absorption components that could lower the emission contribution of the line profile. The higher value of the column density of NH_2CN is confirmed by the analysis of the ^{13}C isotopolog (see Sect. 3.2).

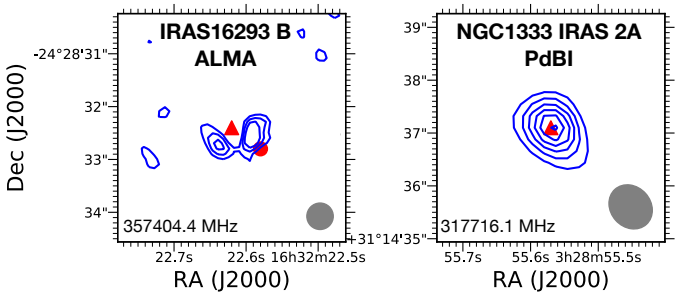

Fig. 1. Integrated intensity maps of two transitions of NH_2CN detected towards IRAS 16293 B (*left panel*, from 3 to 5σ by step of 1σ) and IRAS2A (*right panel*, from 5 to 25σ by step of 5σ). The position of the continuum peak position is indicated with a red triangle, while the position analyzed for IRAS 16293 B (full-beam offset) is indicated with a red circle. The beam size is shown in gray in the bottom right corner.

Three bright and unblended lines of cyanamide are also detected towards NGC 1333 IRAS2A (see Fig. 3). An excitation temperature of ∼130 K and a source size of ∼0.5″ were derived from the analysis of other complex organics towards this source by Coutens et al. (2015). Based on these parameters, a LTE model with a column density of 2.5 × 10^{14} cm^{-2} is in very good agreement with the observations. An excitation temperature of 300 K does not properly reproduce the lines. No other line is missing in the spectral range covered by our data. Based on this model, we can confirm the detection of this molecule by comparing our predictions with the list of lines observed in the spectral range 216.8–220.4 GHz covered by the CALYPSO program (Maury et al. 2014). Among the six brightest lines, five of them are in agreement with the presence of unidentified lines detected by Maury et al. (2014; see Table A.5). The last one is blended with a NH_2CHO line. Maps confirm that the molecule is emitting within the warm inner regions of the source (see Fig. 1).

We also searched for carbodiimide, HNCNH, which is not detected with an upper limit of 3 × 10^{15} cm^{-2} towards IRAS 16293 B. Based on the non-detection of the HNCNH line at 223.7918 GHz, we derived a similar upper limit for IRAS2A. The non-detection of carbodiimide is not really surprising since the upper limits are high and this isomer is known to be less stable than cyanamide.

3.2. Analyses of the deuterated and ^{13}C isotopologs of cyanamide

The ^{13}C and deuterated isotopologs of NH_2CN were searched for towards both sources. Eight unblended lines of NHDCN were identified towards the full-beam offset position of IRAS 16293 B (see Fig. 4). This marks the first detection of this isotopolog in the interstellar medium. Although the lines are faint, we can confirm that all the features are real after checking the spectra at the half-beam position (where the lines are brighter). Additional lines are present, but are not included here as they are blended with other species. A few other lines do not appear as

[1] http://youngstars.nbi.dk/PILS/

[2] CASSIS has been developed by IRAP-UPS/CNRS (http://cassis.irap.omp.eu/).

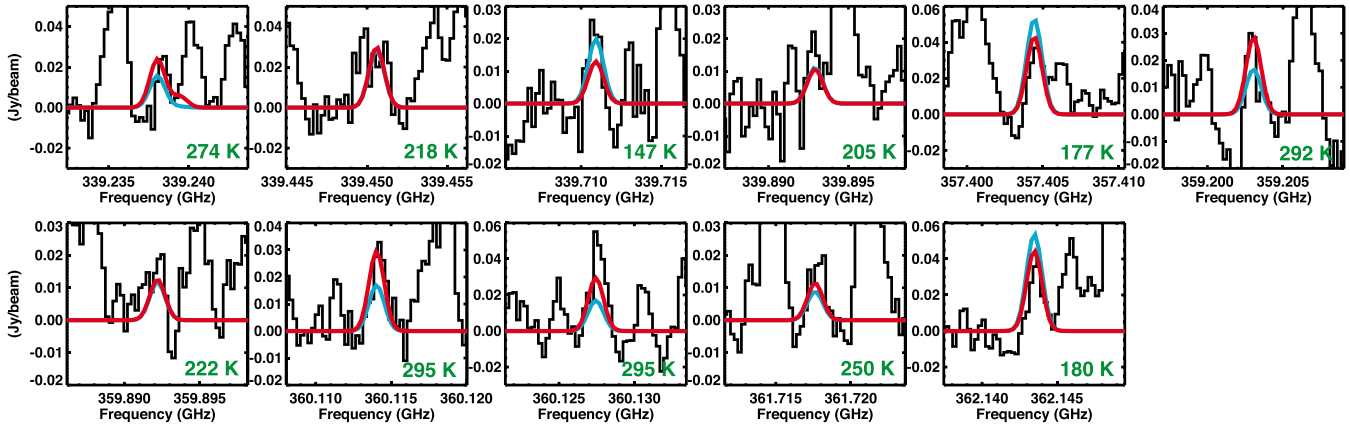

Fig. 2. Unblended lines of NH_2CN detected with ALMA towards IRAS 16293 B at the full-beam offset position. The best-fit model for T_{ex} = 300 K and 100 K are in red and blue, respectively. The E_{up} values are indicated in green in the bottom right corner of each panel.

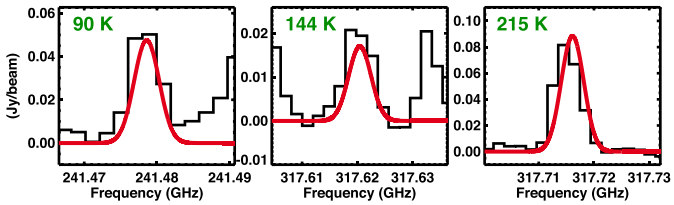

Fig. 3. Unblended lines of NH_2CN detected with PdBI towards IRAS2A. The best-fit model is shown in red. The E_{up} values are indicated in green in the top left corner of each panel.

bright as expected due to the presence of absorptions produced by other species at the same frequency. A column density of 7×10^{13} cm^{-2} is obtained for an excitation temperature of 300 K. The detection of $NH_2{}^{13}CN$ is less straightforward. Three lines can be attributed to this isotopolog (see Fig. 5). One of them (361.997 GHz) may be blended with an unknown species since its flux is higher than predicted by the LTE model. Based on these lines, a column density of 3×10^{13} cm^{-2} is derived showing that the NH_2CN column density is underestimated due to the contribution of the absorptions. The D/H of NH_2CN (corrected for statistics, i.e., divided by 2) is 1.7%, assuming a standard $^{12}C/^{13}C$ of 68 (Milam et al. 2005). This value is very similar to the deuteration of formamide (~2%; Coutens et al. 2016) and also within the range of the D/H of other COMs (~1–8%, Jørgensen et al. 2018; Persson et al. 2018). In the case of a lower $^{12}C/^{13}C$ of 30, which was found for a few COMs in this source (Jørgensen et al. 2016, 2018), the D/H ratio of NH_2CN would be about 4%.

For IRAS2A, an upper limit of 5×10^{13} cm^{-2} is derived for NHDCN, leading to a D/H of ≤10%. The ^{13}C isotopolog also presents an upper limit of 5×10^{13} cm^{-2}, which is equivalent to a $^{12}C/^{13}C$ of ≥5.

3.3. Abundances of cyanamide

Based on the analysis of the $NH_2{}^{13}CN$ isotopolog and the lower limit of the H_2 column density derived by Jørgensen et al. (2016), for IRAS 16293 B we get an abundance of NH_2CN with respect to H_2 of $\lesssim 2 \times 10^{-10}$ at 60 AU from source B. The NH_2CN/NH_2CHO abundance ratio is about 0.2.

Using the H_2 column density derived by Taquet et al. (2015, 5×10^{24} cm^{-2}) for IRAS2A, the abundance with respect to H_2 is about 5×10^{-11}. A simple analysis of the most optically thin NH_2CHO lines covered by our data suggests a column density of about 1.2×10^{16} cm^{-2} assuming a similar excitation temperature of 130 K. This is in agreement with the value determined by Taquet et al. (2015). The ratio of NH_2CN-to-NH_2CHO is consequently about 0.02, an order of magnitude lower than for IRAS 16293 B.

The NH_2CN-to-NH_2CHO ratios derived for the low-mass protostars are similar to the range of values found in Sgr B2 (Belloche et al. 2013, see Table 1). The NH_2CN-to-NH_2CHO ratio in Orion KL seems to be higher (~0.4–1.5, White et al. 2003). This value is, however, more uncertain since it was obtained using only one line of NH_2CHO and assuming different excitation temperatures for the two molecules.

4. Discussion

The formation routes of NH_2CN have only been marginally explored. According to the Kinetic Database for Astrochemistry[3] (KIDA, Wakelam et al. 2012), there are no known gas-phase mechanisms capable of its production. While the reaction $CN + NH_3 \rightarrow NH_2CN + H$ has been proposed (Smith et al. 2004), the theoretical study of Talbi & Smith (2009) suggests that the production of NH_2CN involves large internal barriers, with HCN and NH_2 being the likely products. An experimental study by Blitz et al. (2009) confirms that this reaction proceeds exclusively to HCN + NH_2. Electronic recombination of NH_2CNH^+ may produce NH_2CN, but the only apparent way to form this ion is through protonation of NH_2CN itself. An alternative source of NH_2CN is thus required to explain our observations. Cyanamide could be formed on grain surfaces through the addition of NH_2 and CN radicals. The possible formation of formamide from the same precursor NH_2 (Fedoseev et al. 2016) could explain the similarity of these two species in terms of deep absorption against the strong continuum and the similar deuteration of the two species towards IRAS 16293 B.

To test this hypothesis we ran MAGICKAL, a three-phase chemical kinetics model (Garrod 2013), modified with the grain-surface back-diffusion correction of Willis & Garrod (2017). The model uses a network based on that of Belloche et al. (2017), in which dissociative recombination of NH_2CNH^+ was assumed to produce NH_2CN in 5% of cases. The reaction NH_2 + CN → NH_2CN was added to the grain/ice chemical network, and

[3] http://kida.obs.u-bordeaux1.fr

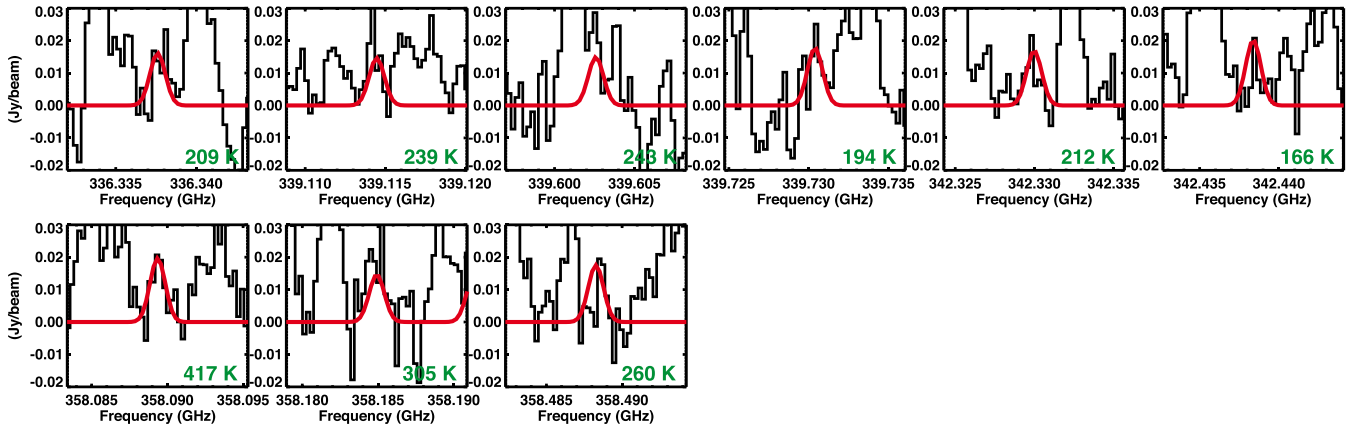

Fig. 4. Unblended lines of NHDCN detected with ALMA towards IRAS 16293 B at the full-beam offset position. The best-fit model for T_{ex} = 300 K is in red. The E_{up} values are indicated in green in the bottom right corner of each panel.

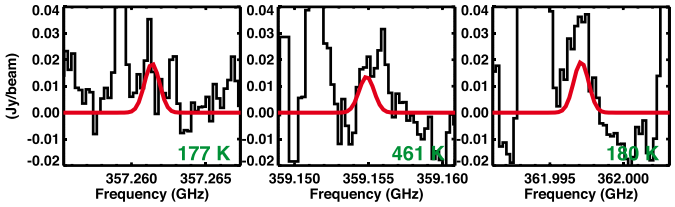

Fig. 5. Lines of $NH_2{}^{13}CN$ detected with ALMA towards IRAS 16293 B at the full-beam offset position. The best-fit model for T_{ex} = 300 K is in red. The E_{up} values are indicated in green in the bottom right corner of each panel.

Table 1. Abundances of NH_2CN with respect to H_2 and NH_2CHO.

Source	NH_2CN/H_2	NH_2CN/NH_2CHO	Telescope
IRAS 16293 B	$\lesssim 2 \times 10^{-10}$ [a]	~0.20	ALMA
NGC 1333 IRAS2A	$\sim 5 \times 10^{-11}$	~0.02	PdBI
Sgr B2 (N)	–	~0.02–0.04	IRAM-30 m
Sgr B2 (M)	–	~0.15	IRAM-30 m
Orion KL	–	~0.4–1.5	JCMT
Low-density model	$\sim 3.7 \times 10^{-10}$	$\sim 1.1 \times 10^{-3}$	
High-density model	$\sim 6.7 \times 10^{-12}$	$\sim 1.3 \times 10^{-4}$	

Notes. [a] Based on the lower limit of 1.2×10^{25} cm^{-2} for the H_2 abundance derived by Jørgensen et al. (2016).

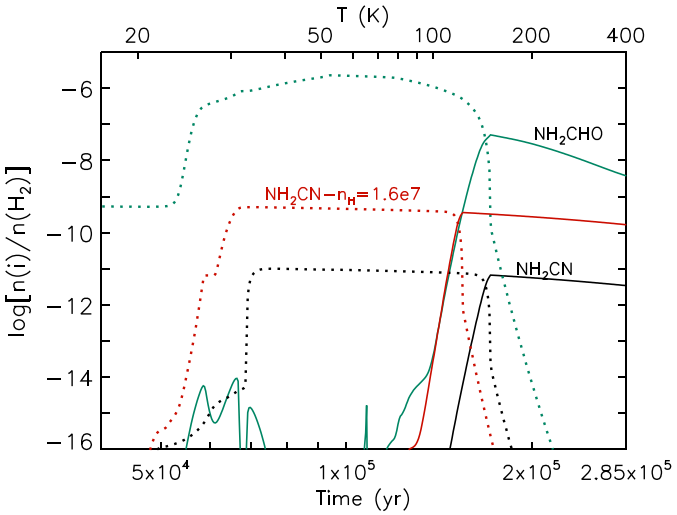

Fig. 6. Chemical model abundances for the warm-up stage of a hot-core type model with a final collapse density of $n_H = 6 \times 10^{10}$ cm^{-3} (high-density model, black lines for NH_2CN and green lines for NH_2CHO). Solid lines denote gas-phase molecules; dotted lines indicate the same species on the grains. The red lines correspond to the abundance profiles of gas-phase and grain-surface NH_2CN for the lower density model, run at $n_H = 1.6 \times 10^7$ cm^{-3}.

the gas-phase reaction between CN and NH_3 was adjusted per Talbi & Smith (2009) and Blitz et al. (2009). The physical model used here is very similar to that described by Belloche et al. (2017), in which a cold collapse to high density is followed by a temperature increase to 400 K; here, a final density $n_H = 6 \times 10^{10}$ cm^{-3} was assumed to better represent the density structure of IRAS 16293 B (Jørgensen et al. 2016).

The model results (for an intermediate warm-up timescale) are shown in Fig. 6 for both NH_2CN and NH_2CHO. $NH_2CN$is seen to be produced at a temperature of ~30 K on the grain surfaces, desorbing into the gas at higher temperatures. The model underproduces the amount of gas-phase NH_2CN, showing a peak fractional abundance with respect to H_2 of $\sim 6.7 \times 10^{-12}$ that is nevertheless well maintained to a temperature of 300 K and beyond. The low NH_2CN abundance in the gas-phase is caused primarily by underproduction on the dust grains; at the high density used in the model, the rapid accretion of H and H_2 onto grain surfaces makes hydrogenation of the NH_2 and CN radicals much more competitive with the reaction that produces NH_2CN. This competition becomes important for gas densities greater than $\sim 10^9$ cm^{-3}. We therefore also present a model with a lower final density of $n_H = 1.6 \times 10^7$ cm^{-3} (corresponding to the density of the envelope between the two protostars in IRAS 16293, Jacobsen et al. 2018), intended to represent the approximate conditions of the gas while at a temperature of 30 K (see Fig. 6). This model produces an NH_2CN fractional abundance of 3.7×10^{-10}, a value very close to the detected value. However, the resulting NH_2CN:NH_2CHO peak abundance ratio of 0.0011 is still lower than the observed values in both IRAS2A (~0.02), and IRAS 16293 (~0.2). This may be due to the possible overproduction of NH_2CHO, related to uncertainties in the efficiency of formation of that molecule, which is still a matter of debate, particularly for the gas-phase mechanism (e.g., Barone et al. 2015; Song & Kästner 2016); our model assumes

only a grain-surface/ice formation route. The difficulty in reproducing the observed NH_2CN abundance at the high densities determined for the source highlights the necessity for future models of hot-core/corino chemistry to treat the rising density and temperature in such cores concurrently, rather than as a two-stage process, so that the gas densities are appropriate at the key temperatures at which many molecules are formed.

In conclusion, the detection of cyanamide towards IRAS 16293 B and IRAS2A indicates that this species can be formed early in solar-type protostars. If it survives during the star formation process until its incorporation into comets or asteroids, these objects could then deliver it to planets, which may enable the development of life. Searches for this species in the coma of comets could shed further light on this possibility. Theoretical and experimental studies as well as more detailed chemical models are needed to confirm the formation of NH_2CN through the grain-surface pathway NH_2 + CN. It would also be interesting to investigate whether this mechanism is sufficient to explain the large-scale emission of NH_2CN in galaxies.

Acknowledgements. This paper makes use of the ALMA data ADS/JAO.ALMA#2013.1.00278.S. ALMA is a partnership of ESO (representing its member states), NSF (USA), and NINS (Japan), together with NRC (Canada) and NSC and ASIAA (Taiwan), in cooperation with the Republic of Chile. The Joint ALMA Observatory is operated by ESO, AUI/NRAO, and NAOJ. This work is based on observations carried out under project numbers V010, V05B, W00A, and X060 with the IRAM Plateau de Bure Interferometer. IRAM is supported by INSU/CNRS (France), MPG (Germany), and IGN (Spain). The research leading to these results has received funding from the European Commission Seventh Framework Programme (FP/2007-2013) under grant agreement No. 283393 (RadioNet3). A.C.'s postdoctoral grant is funded by the ERC Starting Grant 3DICE (grant agreement 336474). The group of J.K.J. acknowledges support from ERC Consolidator Grant "S4F" (grant agreement 646908). Research at the Centre for Star and Planet Formation is funded by the Danish National Research Foundation. The group of E.v.D. acknowledges ERC Advanced Grant "CHEMPLAN" (grant agreement 291141). M.V.P.'s postdoctoral position is funded by the ERC consolidator grant 614264. M.N.D. acknowledges the financial support of the Center for Space and Habitability (CSH) Fellowship and the IAU Gruber Foundation Fellowship.

References

Aladro, R., Martín, S., Martín-Pintado, J., et al. 2011, A&A, 535, A84
Barone, V., Latouche, C., Skouteris, D., et al. 2015, MNRAS, 453, L31
Baryshev, A. M., Hesper, R., Mena, F. P., et al. 2015, A&A, 577, A129
Belloche, A., Müller, H. S., Menten, K. M., Schilke, P., & Comito, C. 2013, A&A, 559, A47
Belloche, A., Meshcheryakov, A. A., Garrod, R. T., et al. 2017, A&A, 601, A49
Birk, M., Winnewisser, M., & Cohen, E. A. 1989, J. Mol. Spectr., 136, 402
Blitz, M. A., Seakins, P. W., & Smith, I. W. M. 2009, Phys. Chem. Chem. Phys., 11, 10824
Bottinelli, S., Ceccarelli, C., Neri, R., et al. 2004, ApJ, 617, L69
Coutens, A., Jørgensen, J. K., Persson, M. V., et al. 2014, ApJ, 792, L5
Coutens, A., Persson, M. V., Jørgensen, J. K., Wampfler, S. F., & Lykke, J. M. 2015, A&A, 576, A5
Coutens, A., Jørgensen, J. K., van der Wiel, M. H. D., et al. 2016, A&A, 590, L6
Duvernay, F., Chiavassa, T., Borget, F., & Aycard, J.-P. 2005, J. Phys. Chem. A, 109, 603
Fedoseev, G., Chuang, K.-J., van Dishoeck, E. F., Ioppolo, S., & Linnartz, H. 2016, MNRAS, 460, 4297
Garrod, R. T. 2013, Astrophys. J., 765, 60
Jabs, W., Winnewisser, M., Belov, S. P., Klaus, T., & Winnewisser, G. 1997, Chem. Phys., 225, 77
Jacobsen, S. K., Jørgensen, J. K., van der Wiel, M. H. D., et al. 2018, A&A, 612, A72
Jørgensen, J. K., Bourke, T. L., Myers, P. C., et al. 2005, ApJ, 632, 973
Jørgensen, J. K., Favre, C., Bisschop, S. E., et al. 2012, ApJ, 757, L4
Jørgensen, J. K., van der Wiel, M. H. D., Coutens, A., et al. 2016, A&A, 595, A117
Jørgensen, J. K., Müller, H. S. P., Calcutt, H., et al. 2018, A&A, submitted
Kahane, C., Ceccarelli, C., Faure, A., & Caux, E. 2013, ApJ, 763, L38
Kilpatrick, M. L. 1947, J. Am. Chem. Soc., 69, 40
Kisiel, Z., Krasnicki, A., Jabs, W., et al. 2013, J. Phys. Chem. A, 117, 9889
Kraśnicki, A., Kisiel, Z., Jabs, W., Winnewisser, B. P., & Winnewisser, M. 2011, J. Mol. Spectrosc., 267, 144
Ligterink, N. F. W., Coutens, A., Kofman, V., et al. 2017, MNRAS, 469, 2219
Lykke, J. M., Coutens, A., Jørgensen, J. K., et al. 2017, A&A, 597, A53
Martín, S., Mauersberger, R., Martín-Pintado, J., Henkel, C., & García-Burillo, S. 2006, ApJS, 164, 450
Martín-Doménech, R., Rivilla, V. M., Jiménez-Serra, I., et al. 2017, MNRAS, 469, 2230
Maury, A. J., Belloche, A., André, P., et al. 2014, A&A, 563, L2
Milam, S. N., Savage, C., Brewster, M. A., Ziurys, L. M., & Wyckoff, S. 2005, ApJ, 634, 1126
Müller, H. S. P., Thorwirth, S., Roth, D. A., & Winnewisser, G. 2001, A&A, 370, L49
Müller, H. S. P., Schlöder, F., Stutzki, J., & Winnewisser, G. 2005, J. Mol. Struct., 742, 215
Persson, M. V., Jørgensen, J. K., van Dishoeck, E. F., & Harsono, D. 2014, A&A, 563, A74
Persson, M. V., Jørgensen, J. K., Müller, H. S. P., et al. 2018, A&A, 610, A54
Pickett, H. M., Poynter, R. L., Cohen, E. A., et al. 1998, J. Quant. Spectr. Radiat. Transf., 60, 883
Raymond, S. N., Quinn, T., & Lunine, J. I. 2004, Icarus, 168, 1
Read, W. G., Cohen, E. A., & Pickett, H. M. 1986, J. Mol. Spectr., 115, 316
Smith, I. W. M., Herbst, E., & Chang, Q. 2004, MNRAS, 350, 323
Song, L., & Kästner, J. 2016, Phys. Chem. Chem. Phys., 18, 29278
Talbi, D., & Smith, I. W. M. 2009, Phys. Chem. Chem. Phys., 11, 8477
Taquet, V., López-Sepulcre, A., Ceccarelli, C., et al. 2015, ApJ, 804, 81
Turner, B. E., Liszt, H. S., Kaifu, N., & Kisliakov, A. G. 1975, ApJ, 201, L149
Wakelam, V., Herbst, E., Loison, J.-C., et al. 2012, ApJS, 199, 21
White, G. J., Araki, M., Greaves, J. S., Ohishi, M., & Higginbottom, N. S. 2003, A&A, 407, 589
Williams, A., & Ibrahim, I. T. 1981, Chem. Rev., 81, 589
Willis, E. R., & Garrod, R. T. 2017, ApJ, 840, 61

Appendix A: Tables with detected lines of NH_2CN and its isotopologs

Table A.1. Detected lines of NH_2CN towards IRAS 16293 B with ALMA.

Transition (N, K_a, K_c, v)	Frequency (MHz)	E_{up} (K)	A_{ij} (s^{-1})	g_{up}
17 2 15 1–16 2 14 1	339238.0	274.3	3.9×10^{-3}	105
17 0 17 1–16 0 16 1	339450.6	218.0	4.04×10^{-3}	105
17 0 17 0–16 0 16 0	339710.9	146.8	4.15×10^{-3}	35
17 2 15 0–16 2 14 0	339892.9	204.8	4.10×10^{-3}	35
18 1 18 0–17 1 17 0	357404.4	177.5	4.82×10^{-3}	111
18 2 16 1–17 2 15 1	359203.0	291.6	4.65×10^{-3}	111
18 2 16 0–17 2 15 0	359892.2	222.0	4.88×10^{-3}	37
18 3 16 0–17 3 15 0	360114.0	294.5	4.87×10^{-3}	111
18 3 15 0–17 3 14 0	360127.4	294.6	4.87×10^{-3}	111
18 1 17 1–17 1 16 1	361717.6	250.4	4.88×10^{-3}	37
18 1 17 0–17 1 16 0	362143.5	179.6	5.02×10^{-3}	111

Table A.2. Detected lines of NH_2CN towards IRAS2A with PdBI.

Transition (N, K_a, K_c, v)	Frequency (MHz)	E_{up} (K)	A_{ij} (s^{-1})	g_{up}
12 1 11 0–11 1 10 0	241478.6	89.8	1.46×10^{-3}	75
16 1 16 1–15 1 15 1	317620.4	215.0	3.29×10^{-3}	33
16 1 16 0–15 1 15 0	317716.1	144.1	3.37×10^{-3}	99

Table A.3. Detected lines of NHDCN towards IRAS 16293 B with ALMA.

Transition (N, K_a, K_c, v)	Frequency (MHz)	E_{up} (K)	A_{ij} (s^{-1})	g_{up}
18 1 18 1–17 1 17 1	336337.6	209.2	3.93×10^{-3}	37
18 2 17 1–17 2 16 1	339114.5	239.4	3.94×10^{-3}	37
18 3 16 0–17 3 15 0	339602.6	243.2	4.07×10^{-3}	37
18 2 16 0–17 2 15 0	339730.4	194.1	4.10×10^{-3}	37
18 1 17 1–17 1 16 1	342330.0	211.9	4.14×10^{-3}	37
18 1 17 0–17 1 16 0	342438.4	166.0	4.24×10^{-3}	37
19 5 15 0–18 5 14 0	358089.4	416.9	4.54×10^{-3}	39
19 5 14 0–18 5 13 0	358089.4	416.9	4.54×10^{-3}	39
19 3 17 1–18 3 16 1	358184.9	304.9	4.63×10^{-3}	39
19 3 16 0–18 3 15 0	358488.3	260.4	4.80×10^{-3}	39

Table A.4. Detected lines of $NH_2{}^{13}CN$ towards IRAS 16293 B with ALMA.

Transition (N, K_a, K_c, v)	Frequency (MHz)	E_{up} (K)	A_{ij} (s^{-1})	g_{up}
18 1 18 0–17 1 17 0	357261.4	177.4	4.82×10^{-3}	111
18 4 15 1–17 4 14 1	359154.9	460.9	4.55×10^{-3}	111
18 4 14 1–17 4 13 1	359154.9	460.9	4.55×10^{-3}	111
18 1 17 0–17 1 16 0	361997.1	179.6	5.01×10^{-3}	111

Table A.5. Unidentified lines from (Maury et al. 2014; their Table 1) that can be assigned to NH_2CN. These data have a spectral resolution of 3.9 MHz (~5.3 km s^{-1}).

Rest frequency (MHz)	Frequency of the U-line (MHz)
218461.8	No U-line but blending with NH_2CHO at 218459 MHz
219441.6	219441
219474.0	219474
219719.7	219719
219893.8	219892
220126.6	220126
220127.9	220126

Appendix B: Spectra of NH_2CN observed with ALMA at different positions towards IRAS 16293 B

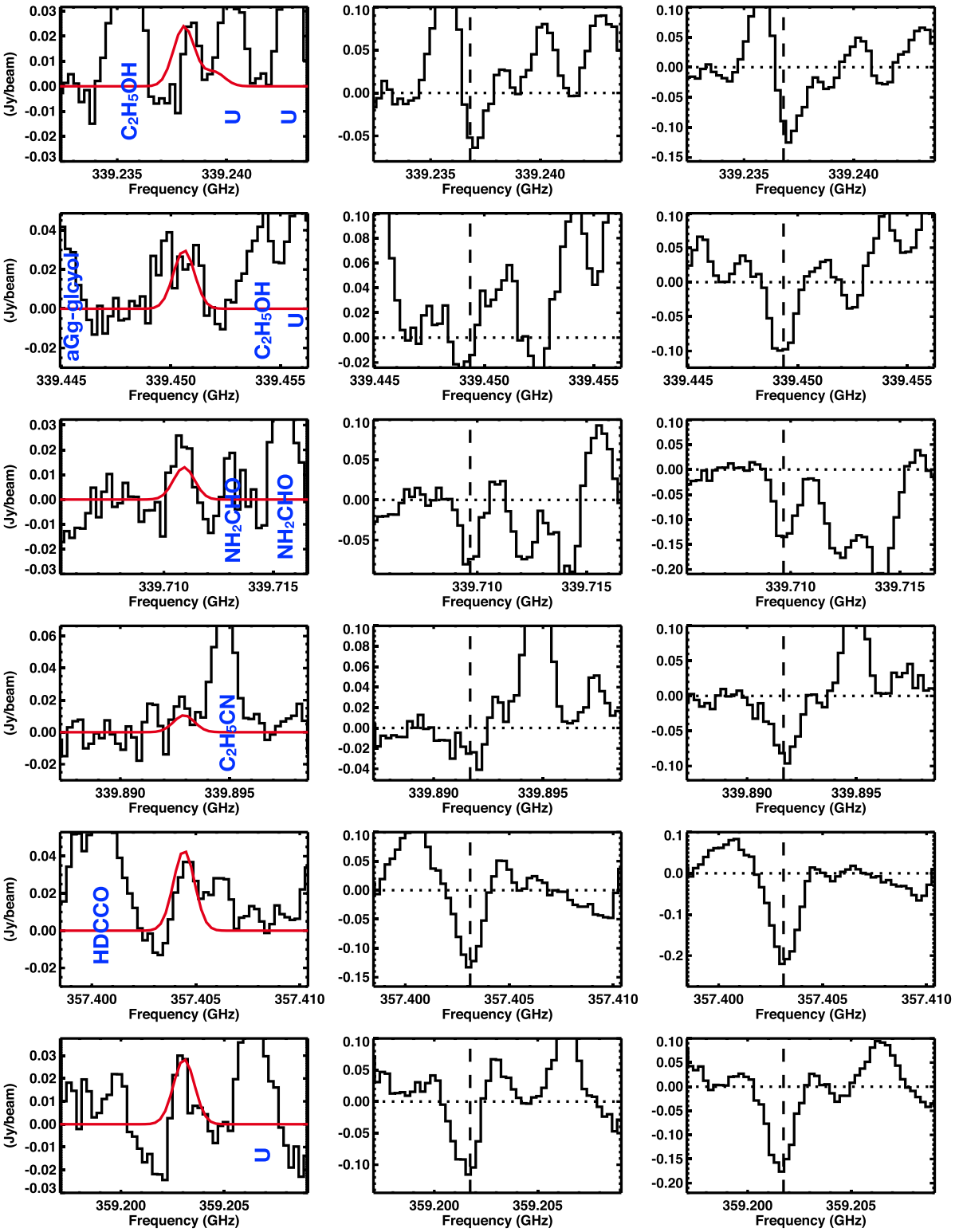

Fig. B.1. Spectra of the unblended lines of NH_2CN detected with ALMA towards IRAS 16293 B at the full-beam offset position (*left*), at the half-beam offset position (*middle*), and at the peak continuum position (*right*). The best-fit model for T_{ex} = 300 K at the full-beam offset position is shown in red in the *left panels*. The identification of the other lines is indicated in blue. The dashed lines in the *middle* and *right panels* indicate the average velocity of the absorptions, 3.8 km s^{-1}. The dotted lines show the level 0.

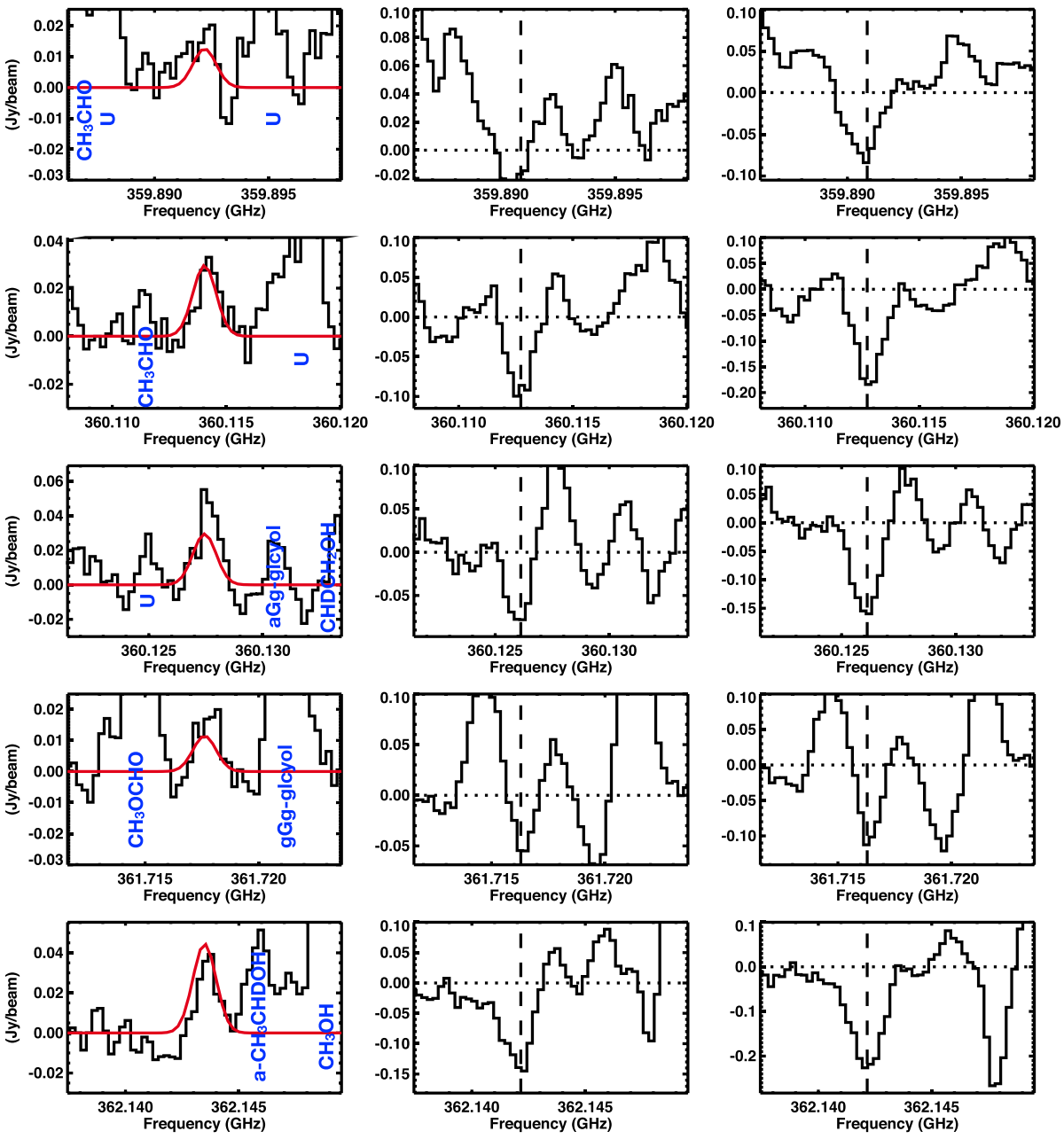

Fig. B.1. continued.